ν = kinematic viscosity μ/ρ
ξ_1 = dimensionless distance y/R at which Equations (2) and (3) coincide
ρ = density of fluid
τ_o = shear stress at the wall

LITERATURE CITED

Astarita, G., "Possible Interpretation of the Mechanism of Drag Reduction," *Ind. Eng. Chem. Fundamentals*, **4**, 354 (1965).

———, and L. Nicodemo, "Extensional Flow Behavior of Polymer Solutions," *Chem. Eng. J.*, **1**, 57 (1970).

Baid, K. M., "Elongational Flows of Dilute Polymer Solutions," Ph.D. thesis, Univ Del., Newark (1973).

Bakewell, H. P., Ph.D. thesis, Pa. State Univ., University Park, (1966).

Batchelor, G. K., "The Stress Generated in a Non-Dilute Suspension of Elongated Particles by Pure Straining Motion," *J. Fluid Mech.*, **46**, 813 (1971).

Blatch, N. S., "Water Filtration at Washington," *Trans. A.S.C.E.*, **57**, 400 (1906).

Bobkowicz, A. J., and W. H. Gauvin, "The Turbulent Flow Characteristics of Model Fiber Suspensions," *Can. J. Chem. Eng.*, **43**, 87 (1965).

Brecht, W., and H. Heller, "A Study of the Pipe Friction Losses of Paper Stock Suspensions," *TAPPI*, **33**, 14A (1950).

Daily, J. W., and G. Bugliarello, "Basic Data for Dilute Fiber Suspensions in Uniform Flow with Shear," *TAPPI*, **44**, 497 (1961).

Denn, M. M. and G. Marrucci, "Stretching of Viscoelastic Fluids," *AIChE J.*, **17**, 101 (1971).

Dodge, D. W., and A. B. Metzner, "Turbulent Flow of Non-Newtonian Systems," *ibid.*, **5**, 189 (1959).

Elata, C., J. Lehrer, and A. Kahanovitz, "Turbulent Shear Flow of Polymer Solutions," *Israel J. Tech.*, **4**, 87 (1966).

Forrest, F., and G. A. H. Grierson, "Friction Losses in Cast Iron Pipe Carrying Paper Stock," *Paper Trade J.*, **298** (1931).

Gadd, G. E., "Turbulence Damping and Drag Reduction Produced by Certain Additives," *Nature*, **463**, 206 (1965).

Hansen, R. J., "The Reduced Drag of Polymer Solutions in Turbulent and Transient Laminar Shear Flows," *Trans. A.S.M.E. (J. Fluids Eng.)*, **95**, 23 (1973).

Hoyt, J. W., "The Effect of Additives on Fluid Friction," *Trans. A.S.M.E. (J. Basic Eng.)*, **94 D**, 258 (1972*a*).

———, "Turbulent Flow of Drag Reducing Suspensions," *Naval Undersea Center Rept. TP 299*, San Diego, Calif. (1972*b*).

Kale, D. D., and A. B. Metzner, "Turbulent Drag Reduction in Fiber-Polymer Systems: Specificity Consideration," *AIChE J.*, **20**, 1218 (1974).

Kenis, P. R., "Drag Reduction by Bacterial Metabolites," *Nature*, **217**, 940 (1968).

Kerekes, R. J. E., and W. J. M. Douglas, "Viscosity Properties of Suspensions at the Limiting Conditions for Turbulent Drag Reduction," *Can. J. Chem. Eng.*, **50**, 228 (1972).

Kizior, T. E., and F. A. Seyer, "Axial Stress in Elongational Flow of Fiber Suspension," *Trans. Soc. Rheology*, **18**, 271 (1974).

Lee, W. K., R. C. Vaseleski, and A. B. Metzner, "Turbulent Drag Reduction in Polymeric Solutions Containing Suspended Fibers," *AIChE J.*, **20**, 128 (1974). See also *U. S. Patent 3,938,536* (1976).

Little, R. C., et al., "The Drag Reduction Phenomenon. Observed Characteristics, Improved Agents and Proposed Mechanisms," *Ind. Eng. Chem. Fundamentals*, **14**, 283 (1975).

Lornston, J. M., "Extensional Flows of Molten Polyethylene," M.Ch.E. thesis, Univ. Del., Newark (1975).

Metzner, A. B., and A. P. Metzner, "Stress Levels in Rapid Extensional Flows of Polymeric Fluids," *Rheologica Acta*, **9**, 174 (1970).

Metzner, A. B., and M. G. Park, "Turbulent Flow Characteristics of Viscoelastic Fluids," *J. Fluid Mech.*, **20**, 291 (1964).

Mewis, J., and A. B. Metzner, "The Rheological Properties of Suspensions of Fibers in Newtonian Fluids Subjected to Extensional Deformations," *ibid.*, **62**, 593 (1974).

Meyer, W. A.., "A Correlation of the Frictional Characteristics for Turbulent Flow of Dilute Viscoelastic Non-Newtonian Fluids in Pipes," *AIChE J.*, **12**, 522 (1966).

Mih, W. and J. Parker, "Velocity Profile Measurements and a Phenomenological Description of Turbulent Fiber Suspension Pipe Flow," *TAPPI*, **50**, 237 (1967).

Radin, I., J. L. Zakin, and G. K. Patterson, "Drag Reduction in Solid-Fluid Systems," *AIChE J.*, **21**, 358 (1975).

Ruckenstein, E., "On the Mechanism of Drag Reduction in Turbulent Flow of Viscoelastic Liquids," *Chem. Eng. Sci.*, **26**, 1075 (1971).

Rudd, M. J., "Measurements Made on a Drag Reducing Solution with a Laser Velocimeter," *Nature*, **224**, 587 (1969).

Savins, J. G., "A Stress Controlled Drag Reduction Phenomenon," *Rheologica Acta*, **6**, 323 (1967).

———, "Contrasts in the Solution Drag Characteristics of Polymeric Solutions and Micellar Systems," in *Viscous Drag Reduction*, C. S. Wells, ed., p. 183, Plenum Press, New York (1969).

Schlichting, H., *Boundary Layer Theory*, Chapt. 20, McGraw Hill, New York (1968).

Seyer, F. A., and A. B. Metzner, Proc. 6th Symp. on Naval Hydrodynamics, Dept. of the Navy, Washington (1966). See also *Can. J. Chem. Eng.*, **45**, 121 (1967).

———, "Turbulence Phenomena in Drag Reducing Systems," *AIChE J.*, **15**, 426 (1969).

Vaseleski, R. C., and A. B. Metzner, "Drag Reduction in the Turbulent Flow of Fiber Suspensions," *ibid.*, **20**, 301 (1974).

Virk, P. S., "Drag Reduction Fundamentals (Journal Review)," *ibid.*, **21**, 625 (1975).

Manuscript received August 6, 1975; revision received and accepted March 22, 1976.

A Flow Model for Gas Movement in Spouted Beds

A two-region model of a spouted bed, postulating vertical plug flow of gas in the spout and dispersed plug flow along curved streamlines in the annulus, is proposed. The extent of axial dispersion is accounted for by a coefficient D which is an adjustable parameter of the model. Experimental support for the theory is provided by residence time-distribution data obtained by using helium gas as tracer, covering a wide range of conditions. Values of the coefficient D, determined from a comparison between predicted and observed RTD curves, are generally higher than those reported for packed beds but much smaller than those for fluidized beds.

C. J. LIM

and

K. B. MATHUR

Department of Chemical Engineering
University of British Columbia
Vancouver, B.C.

SCOPE

The spouted bed technique for contacting a fluid with coarse granular solids has attracted attention for a variety of applications (Mathur and Epstein, 1974), some involving heat and/or mass transfer (drying, granulation,

particle coating, gas cleaning, etc.) or chemical reaction (for example, coal carbonization, shale pyrolysis, iron ore reduction, and petroleum cracking). For scale-up and design of spouted bed reactors for such applications, it is necessary that the detailed movement of the fluid in the reactor should be understood and related to the system variables through a mathematical model.

The first attempt to develop such a model was made by the present authors (Lim and Mathur, 1974), assuming that gas moves vertically upwards in the spout as well as the annulus, in plug flow in the former region and in axially dispersed plug flow in the latter. While RTD measurements made in 15 cm diameter beds of several solid materials were consistent with the model, further tests, especially in larger columns (24 and 29 cm diam.), revealed noticeable differences between response curves at different radial positions across the annulus surface. These differences can not be accounted for by our simplified model, since the assumption of vertical plug flow in the annulus implies radial uniformity of gas residence time.

The work reported in this paper was carried out with the object of developing a gas flow model based on a more realistic description of the flow pattern in the annulus and supported by experimental data covering a wider range of variables, including column diameter.

CONCLUSIONS AND SIGNIFICANCE

The gas flow model now presented takes into account the actual path followed by the gas in the annulus instead of assuming that the gas flows vertically upwards, thus constituting a more accurate description of physical behavior than our earlier simplified model. The revised theory is well supported by RTD measurements carried out by using helium gas as tracer, covering a wide range of experimental conditions. Values of the single adjustable model parameter D, which represents dispersion along flow lines in the annulus, show reasonable trends with the variables studied and are higher than for packed beds but much smaller than for fluidized beds.

The model proposed should provide a sound basis for analyzing spouted bed performance with respect to heat and mass transfer, and chemical reaction, as well as for scale-up and design purposes.

PRELIMINARY OBSERVATIONS

Visual observation in a half-sectional column with nitrogen dioxide used as tracer showed that in the spouted bed annulus, gas travels radially as well as vertically, but without any perceptible radial dispersion or mixing (see Figure 1). Cross flowing gas at the bottom of the spout was seen to penetrate deeper towards the column wall and then to flow upwards along the wall to the surface of the bed. With the above pattern of flow, the length of the flow path in the annulus becomes smaller with increasing radial distance from the column wall, and this is reflected in helium tracer response curves measured at different radial positions across the annulus surface (Figure 7). Radial variation in residence time became more pronounced with increasing column diameter, and it was

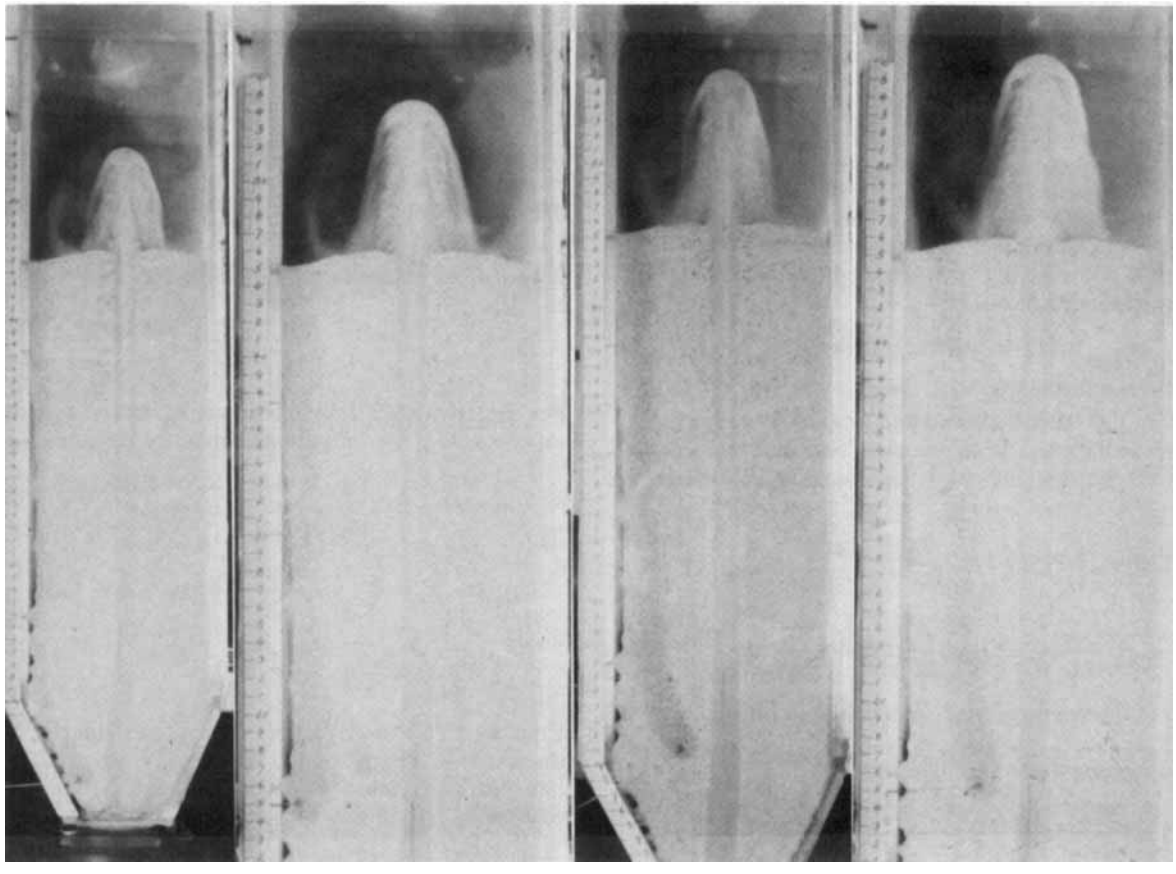

Fig. 1. Streamlines of nitrogen dioxide tracer in a half-sectional spouted bed. Solid material—Ottawa sand, −20 +30 mesh.

therefore realized that in order to be of practical value for design of large scale equipment, the model must take into account the flow pattern described above.

THEORETICAL MODEL

Equations for calculating the residence-time distribution of tracer gas passing through the annulus are developed below, assuming that gas in the spouted bed annulus travels along streamlines described by Equation (1), that no dispersion or mixing occurs in the direction normal to the streamlines, that dispersion along the streamline is represented by a dispersion coefficient D, and that spout gas moves in plug flow and therefore has a radially uniform tracer concentration. The main point of difference between the present model and our previous model (Lim and Mathur, 1974) is in the first assumption above, which replaces the earlier assumption of vertically upward flow in the annulus.

Gas Flow Path

For calcluating the gas flow path in the annulus, we divide the vertical height of the annulus into M equal intervals and the width of the annulus at the top into N equal intervals. Let each interval at the annulus top represent one path of gas flow (see Figure 2), and let $Q(J-1)$ be the volumetric flow rate between streamlines $J-1$ and J.

Gas mass balance at any level I gives

$$Q(J-1) = U_a(I)\,\pi\,[R(J-1,I)^2 - R(J,I)^2] \quad (1)$$

where $U_a(I)$ is the upward superficial gas velocity at level I and $R(J,I)$ the radial distance from the column axis to the intersection between the J^{th} streamline and I. Equation (1) describes the gas streamlines which can be calculated by using experimental values of $U_a(I)$ obtained from static pressure measurements. The outcome of such a calculation, starting from the top of the annulus and ending at the spout-annulus interface, is shown in Figure 3. It was assumed that the first streamline ($J = 1$) coincides with the column wall, as suggested by visual observation of nitrogen dioxide tracer movement (Figure 1). The computed flow pattern in Figure 3 is seen to be generally similar to that observed visually. In order to determine the gas velocity along each streamline, the angle θ formed between the streamline and the vertical axis was measured (see Figure 2), and $u_z(I)$ was calculated by using the following relationship:

$$u_z(I) = U_a(I)/(\epsilon_a \cos\theta) \quad (2)$$

Residence-Time Distribution

Consider the control zone Δz in Figure 4 which represents a vertical section of the annulus between two streamlines. From conservation of tracer for the control zone, we get

$$A\,\epsilon_a \frac{\partial C_a}{\partial t}\,dz = \left[\, C_a\,Q(J) - \left(C_a + \frac{\partial C_a}{\partial z}\,dz\right)Q(J)\,\right] - \left[\, D\,\epsilon_a\,A\frac{\partial C_a}{\partial z} - D\,\epsilon_a\,A\frac{\partial}{\partial z}\left(C_a + \frac{\partial C_a}{\partial z}\,dz\right)\right] \quad (3)$$

where A is the average cross-sectional area between levels I and $I+1$.

Equation (3) can be simplified to

$$A\,\epsilon_a \frac{\partial C_a}{\partial t} = -\frac{Q(J)}{L}\frac{\partial C_a}{\partial z'} + \frac{AD}{L^2}\,\epsilon_a \frac{\partial^2 C_a}{\partial z'^2} \quad (4)$$

where $z' = z/L$, L being the length of the gas flow path. Since $Q(J)/\epsilon_a A$ equals u_z, the average interstitial velocity

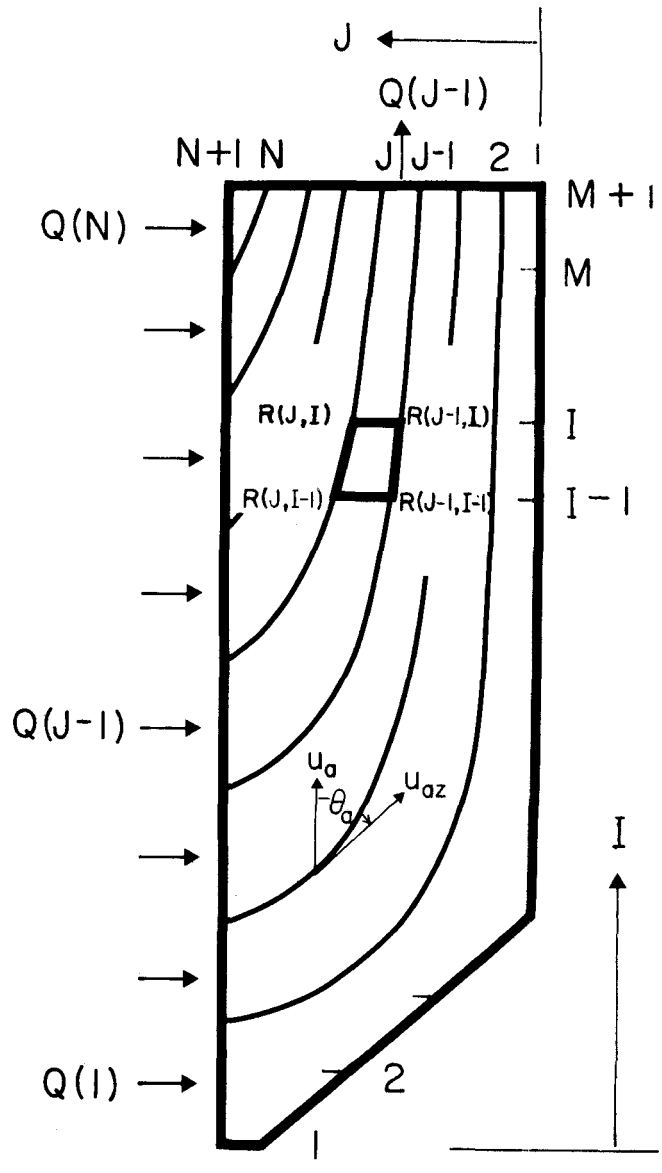

Fig. 2. Coordinate system and grid points for streamline calculations.

between the streamlines, Equation (4) may be rewritten as

$$\frac{\partial C_a}{\partial t} = -\frac{u_z}{L}\frac{\partial C_a}{\partial z'} + \frac{D}{L^2}\frac{\partial^2 C_a}{\partial z'^2} \quad (5)$$

For negative step function input of tracer (used in the experiments), the initial and boundary conditions are

$$\text{for} \quad t \leq 0, \quad C_a = 1.0 \quad (6)$$

$$\text{for} \quad t > 0,$$

$$\text{at} \quad z' = 0, \quad \frac{D}{L}\frac{\partial C_a}{\partial z'} = u_z\,(C_a - C_s) \quad (7)$$

$$\text{at} \quad z' = 1.0, \quad \frac{\partial C_a}{\partial z'} = 0 \quad (8)$$

Equations (5) to (8) apply to any particular gas path in the annulus. For N paths, we have N set of these equations, for each value of J between 1 and N, which may be written as

$$\frac{\partial C_a(J)}{\partial t} + \frac{u_z(J)}{L(J)}\cdot\frac{\partial C_a(J)}{\partial z'} - \frac{D}{L(J)^2}\frac{\partial^2 C_a(J)}{\partial z'^2} = 0 \quad (9)$$

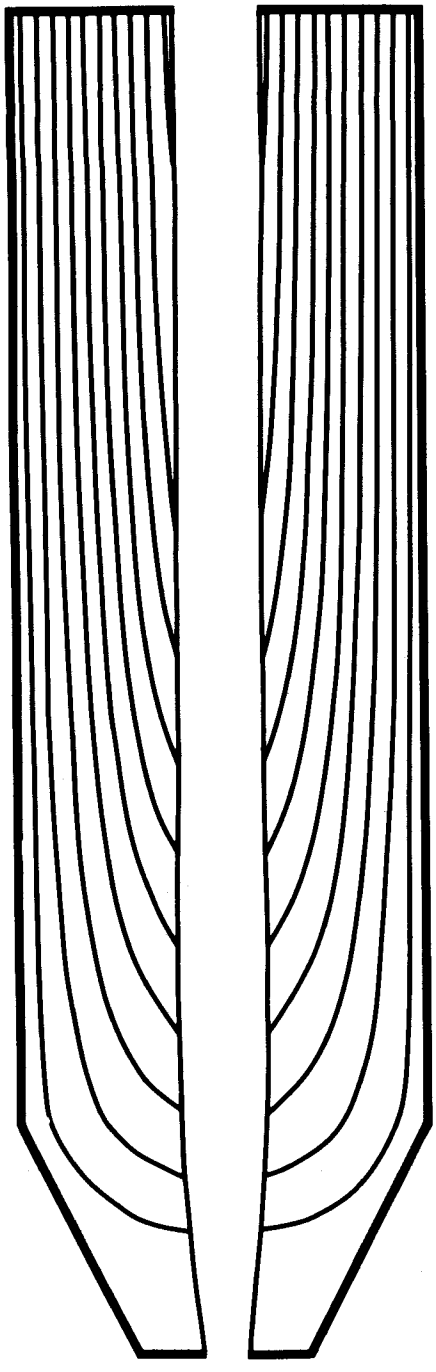

Fig. 3. Calculated streamlines for a 0.24 m diam × 0.72 m deep bed of polystyrene pellets ($D_i/D_c = 0.12$, $U_s/U_{ms} = 1.1$, $d_p = 2.93$ mm).

$$\text{for} \quad t \leq 0, \quad C_a(J) - 1.0 = 0 \tag{10}$$

$$\text{for} \quad t > 0$$

$$\text{at} \quad z' = 0$$

$$\frac{D}{L(J)} \frac{\partial C_a(J)}{\partial z'} - u_z(J)\,[C_a(J) - C_s(J)] = 0 \tag{11}$$

$$\text{at} \quad z' = 1.0$$

$$\frac{\partial C_a(J)}{\partial z'} = 0 \tag{12}$$

In order to solve the above set of equations, an expression for C_s, which appears in Equation (11), is required. Tracer mass balance over a differential height of the spout dz (see Figure 5), by assuming plug flow of spout gas and

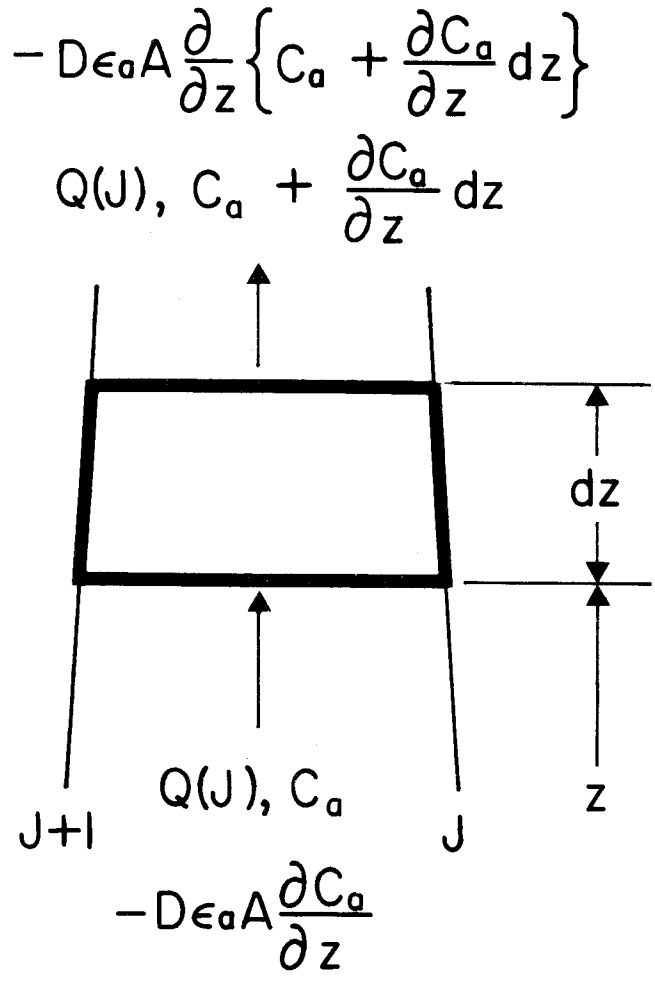

Fig. 4. Tracer mass balance in the annulus.

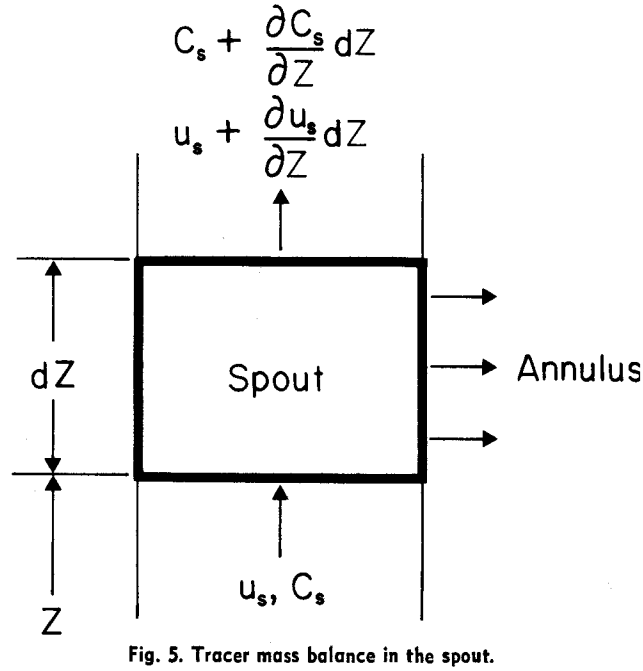

Fig. 5. Tracer mass balance in the spout.

radial uniformity of tracer concentration, gives

$$\frac{\partial C_s}{\partial t} + \frac{u_s}{H} \frac{\partial C_s}{\partial Z'} = 0 \tag{13}$$

u_s being the interstitial upward gas velocity in the spout and Z' the dimensionless bed level Z/H. The relevant initial and boundary conditions are

Table 1. Values of the Dispersion Coefficient D for Spouted Beds and Corresponding Experimental Conditions
(Cone angle—60° deg. included)

No.	Material	D_c, m	D_i/D_c	H/D_c	dp., mm	U_{ms}, m/s	U_s/U_{ms}	H/H_{max}	D, m²/s
1	Polystyrene pellets	0.152	0.125	3.00	2.93	0.82	1.1	0.51	0.024
2	$\rho_s = 1.05$ g/cm³	0.152	0.125	3.00	2.93	0.82	1.2	0.51	0.024
3	$\epsilon_a = 0.41$	0.152	0.125	3.00	2.93	0.82	1.3	0.51	0.025
4	$U_{mf} = 0.63$ m/s	0.152	0.125	2.00	2.93	0.79	1.1	0.34	0.008
5		0.152	0.125	2.00	2.93	0.79	1.2	0.34	0.007
6		0.152	0.125	2.00	2.93	0.79	1.3	0.34	0.008
7		0.152	0.084	3.00	2.93	0.78	1.1	0.48	0.017
8		0.152	0.167	3.00	2.93	0.88	1.1	0.55	0.018
9		0.241	0.120	3.00	2.93	0.75	1.1	0.55	0.016
10		0.292	0.125	3.10	2.93	0.58	1.1	0.51	0.017
11		0.292	0.087	3.10	2.93	0.61	1.1	0.43	0.022
12	Polystyrene pellets, small $\rho_s = 1.05$ g/cm³ $\epsilon_a = 0.49$; $U_{mf} = 0.47$ m/s	0.152	0.125	3.00	1.61	0.52	1.1	0.55	0.011
13	Wheat	0.152	0.125	3.00	3.50	1.08	1.1	0.72	0.021
14		0.152	0.125	3.00	3.50	1.08	1.3	0.72	0.020
15	$\rho_s = 1.24$ g/cm³	0.152	0.125	2.00	3.50	1.00	1.1	0.48	0.017
16	$\epsilon_a = 0.44$	0.152	0.125	1.00	3.50	0.72	1.1	0.24	0.015
17	$U_{mf} = 0.92$ m/s	0.241	0.120	3.00	3.50	0.94	1.1	0.61	0.029
18		0.292	0.125	3.10	3.50	0.82	1.1	0.55	0.017
19		0.292	0.125	1.57	3.50	0.68	1.1	0.28	0.010
20	Millet	0.152	0.125	3.00	2.15	0.67	1.1	0.95	0.013
21	$\rho_s = 1.18$ g/cm³	0.152	0.125	3.00	2.15	0.67	1.3	0.95	0.014
22	$\epsilon_a = 0.42$, $U_{mf} = 0.62$ m/s	0.152	0.084	3.00	2.15	0.62	1.1	0.93	0.014
23	Glass beads	0.152	0.125	2.60	2.93	1.87	1.1	0.94	0.044
24	$\rho_s = 2.94$ g/cm³ $\epsilon_a = 0.42$, $U_{mf} = 1.63$ m/s	0.152	0.125	2.60	2.93	1.87	1.3	0.94	0.044
25	Glass beads, small $\rho_s = 2.96$ g/cm³ $\epsilon_a = 0.41$, $U_{mf} = 0.80$ m/s	0.152	0.125	2.60	1.10	0.72	1.1	0.75	0.003
26	Ammonium nitrate $\rho_s = 1.75$ g/cm³ $\epsilon_a = 0.46$, $U_{mf} = 0.80$ m/s	0.152	0.125	3.00	1.99	0.97	1.1	0.86	0.007
27	Ammonium nitrate, small $\rho_s = 1.74$ g/cm³ $\epsilon_a = 0.44$, $U_{mf} = 0.56$ m/s	0.152	0.125	3.00	1.45	0.68	1.1	0.93	0.005

$$\text{for} \quad t \leq 0, \quad C_s = 1.0 \tag{14}$$

$$\text{for} \quad t > 0, \quad C_s = C_1 \tag{15}$$

The solution of Equation (13) with Laplace transformation used is

$$C_s = \delta(t) - \delta\left[t - \int_o^{Z'} \frac{H}{u_s} dZ'\right] + C_1\left[t - \int_o^{Z'} \frac{H}{u_s} dZ'\right] \times \delta\left[t - \int_o^{Z'} \frac{H}{u_s} dZ'\right] \tag{16}$$

where $\delta(t)$ is the unit step function, $\delta(t < 0) = 0$ and $\delta(t \geq 0) = 1$.

Equations (1) and (2) together with Equations (9), (10), (11), (12), and (16) constitute the theoretical model and can be solved numerically to yield C_a as a function of time (that is, the RTD curve) for any location in the bed. The hydrodynamic data required are longitudinal profiles of U_a, U_s, ϵ_s, and D_s. The dispersion coefficient D in Equations (9) and (11) is the only adjustable parameter of the model, and this will be evaluated for each experiment from a comparison between predicted and observed RTD curves.

EXPERIMENTAL

Particulars of the apparatus and materials used are given in Table 1. Annulus gas velocities for the cylindrical part of the bed were determined from static pressure measurements at the column wall, and for the conical part from spout gas velocities measured with a pitot tube probe. Spout diameters and spout particle velocities were determined in half-round columns by using cine photography, and spout voidages were estimated from data on downward particle velocity at wall and upward velocity in spout. Measurements of residence-time distribution were carried out by injecting helium into the gas approach pipe as a negative step function and by recording the tracer concentration of inlet and exit gas simultaneously with a pair of conductivity cells connected to an oscilloscope. Details of the apparatus used and experimental procedures employed have been described elsewhere (Lim and Mathur, 1974; Lim, 1975).

RESULTS AND DISCUSSION

An example of an experimental RTD curve is shown in Figure 6, which also includes a series of predicted curves for four different values of D. All the curves shown refer to a location halfway across the width of the annulus, immediately above the bed surface. It is seen that for a D value of 0.016 m²/s, the predicted curve gives a very close fit with the experimental curve over the entire range of residence time. All the data obtained in this investigation showed similar agreement with model prediction, the value of D required to obtain the best fit, being variable and dependent on experimental conditions. The method used for obtaining the best fit was to minimize the sum of squared deviation between predicted and observed values over the full range of the response curve.

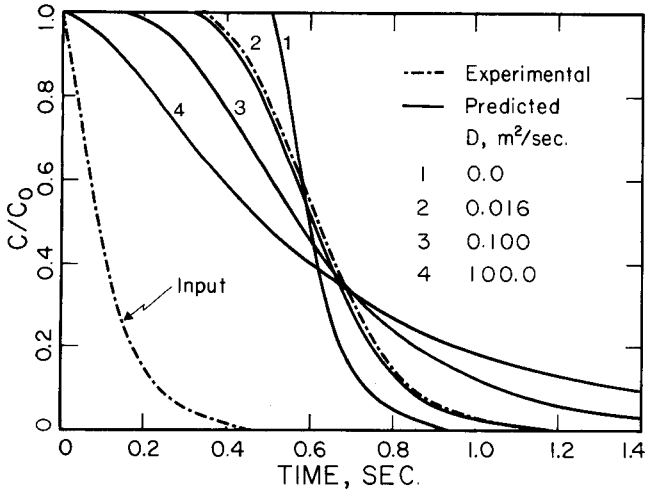

Fig. 6. RTD curves for the system of Figure 3, for a point halfway across the annulus surface.

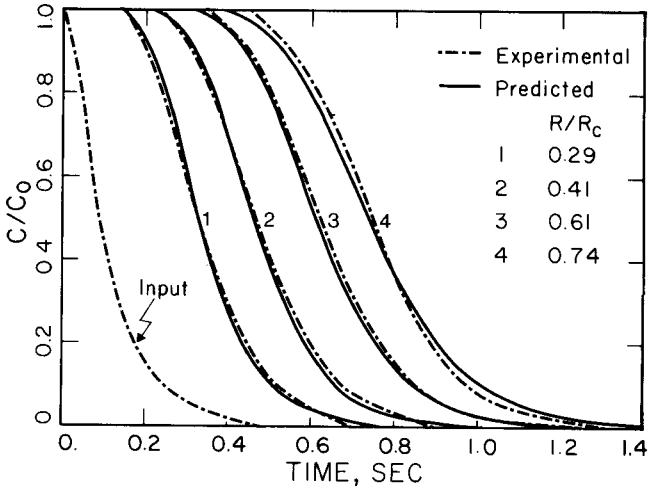

Fig. 7. RTD curves for the system of Figure 6, for different radial positions across the annulus surface.

The series of response curves in Figure 7 was recorded at different radial positions across the annulus surface and illustrates the large radial variations in residence time which occur in the spouted bed annulus. These are predictable from the proposed model, as shown in Figure 7. All the predicted curves in the figure are based on a common value of D (0.016 m²/s) which was arrived at by matching the predicted and observed curves for a single location (midpoint of annulus surface). Figure 7 shows that response curves for other radial locations are also correctly predicted by the model, without any alteration of the D value. This agreement provides strong support for the validity of the theoretical model, and in particular for the procedure for taking the gas flow path into account.

A compilation of all the D values obtained in this work is presented in Table 1, together with the main experimental conditions for each run. The data show that the value of D increases with increasing particle size (run numbers 12 and 1, 25 and 23) and bed depth (4 and 1, 16 and 13, 19 and 18), shows only weak dependence on column diameter (1, 9, 10; 13, 17, 18) and orifice diameter (1 and 7, 10 and 11), and is substantially independent of spouting velocity (1, 2, 3; 4, 5, 6; 20, 21; 23, 24). All these trends can be explained, though only qualitatively, in terms of the gas velocity in the annulus on the premise that in packed beds, axial dispersion is more pronounced at higher gas velocities (Urban and Gomezplata, 1969; Gunn, 1969). Since U_{ms}, and hence the average value of U_a, would increase with increasing d_p as well as with increasing H, the dispersion coefficient D would also be expected to increase. The weak dependence of D on D_c and D_i for geometrically similar beds can be attributed to the weak effect of both these variables on U_a (Mathur and Epstein, 1975, p. 56), while increasing the spouting velocity above U_{ms} would not affect U_a and therefore D, since the excess gas $U_s - U_{ms}$ is known to travel preferentially through the spout region (Mathur and Epstein, 1975, p. 49). In addition to the variables discussed, the characteristics of the solid material, for example, shape and surface properties, probably have an influence on D (Urban and Gomezplata, 1969), but this is difficult to isolate from the data in Table 1. Also, there appears to be no clear trend in D values with the parameter H/H_{max}, which has been used successfully to correlate certain other aspects of spouted bed behavior, namely pressure drop and fluid distribution (Grbavčić et al., 1976).

An attempt to see how axial dispersion in spouted beds compares with that in packed beds and fluidized beds is presented in Figure 8. An accurate comparison is difficult to make, since the gas velocity in the spouted bed annulus,

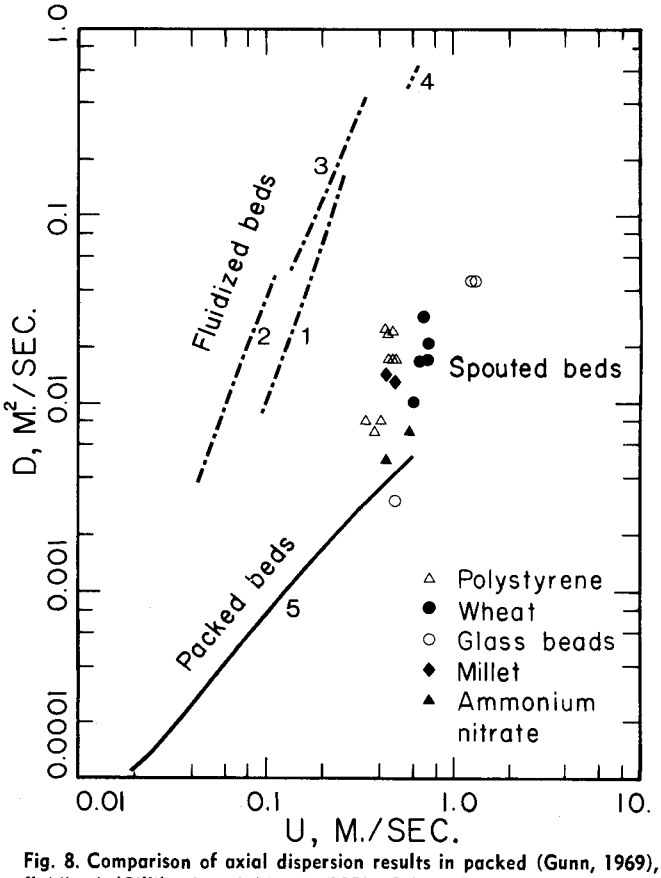

Fig. 8. Comparison of axial dispersion results in packed (Gunn, 1969), fluidized (Gilliland and Mason, 1952; Schügerl, 1967) and spouted beds. [d_p for (1): 0.1-0.16 m, (2): 0.11 mm, (3): 0.25 mm, (4): 0.5 mm, (5): 6 mm.]

unlike that in packed and fluidized beds, changes along the height of the bed. The velocities used for plotting the spouted bed data in Figure 8 are integrated average values over the gas flow path terminating at the midpoint of the annulus surface. The comparison shows that values of D for spouted beds are generally higher than for packed beds (Gunn, 1969), the difference being more pronounced for larger spouted bed particles. When compared with the data for fluidized beds, (Gilliland and Mason, 1952; Schügerl, 1967), the spouted bed results are seen to be at least an order of magnitude smaller.

ACKNOWLEDGMENT

We are grateful to Dr. Norman Epstein for his advice and comments on this work and to the National Research Council of Canada for financial support.

NOTATION

A = cross-sectional area of annulus, m^2
C = tracer concentration at $t \geq 0$
C_o = tracer concentration at $t \leq 0$
C_1 = input tracer concentration, dimensionless
C_a = concentration of tracer in annulus, dimensionless
C_s = concentration of tracer in spout, dimensionless
D = dispersion coefficient, m^2/s
D_c = column diameter, m
D_i = gas inlet diameter, m
D_s = spout diameter, m
d_p = particle diameter, mm, taken as diameter of equivolume sphere
H = bed depth, m
H_{max} = maximum spoutable bed depth, m
I = horizontal grid lines in Figure 2
J = gas streamlines in Figure 2
L = length of flow path in annulus, m
M = number of divisions of H in Figure 2
N = number of streamlines in the annulus in Figure 2
$Q(J-1)$ = flow rate between streamlines $J-1$ and J in the annulus, m^3/s
R = radial distance from spout axis, m
R_c = column radius, m
t = time, s
U = superficial fluid velocity, m/s
U_a = superficial gas velocity in the annulus, m/s
U_{mf} = minimum fluidization velocity, m/s
U_{ms} = minimum spouting velocity, superficial, m/s
U_s = operating spouting velocity, superficial, m/s
u_s = interstitial gas velocity in the spout, m/s
u_z = interstitial gas velocity along the streamline in the annulus, m/s
Z = vertical distance from gas inlet orifice
z = linear distance along a streamline, starting from spout-annulus interface
z' = z/L
Z' = Z/H
ϵ_s = spout voidage
ϵ_a = annulus voidage
$\delta(t)$ = unit step function in Equation (16)
ρ_s = particle density, g/cm^3

LITERATURE CITED

Gilliland, E. R., and E. A. Mason, "Gas Mixing in Beds of Fluidized Solids," *Ind. Eng. Chem.*, 44, 218 (1952).

Grbavčić, Ž., D. V. Vuković, F. K. Zdanski, and H. Littman, "Fluid Flow Pattern, Minimum Spouting Velocity and Pressure Drop in Spouts and Beds," *Can. J. Chem. Eng*, **54**, 33 (1976).

Gunn, D. J., "Theory of Axial and Radial Dispersion in Packed Beds," *Trans. Inst. Chem. Engrs.*, 47, T341 (1969).

Lim, C. J., "Gas Residence Time Distribution and Related Flow Patterns in Spouted Beds," Ph.D. thesis, Univ. British Columbia, Vancouver (1975).

———, and K. B. Mathur, "Residence Time Distribution of Gas in Spouted Beds," *Can. J. Chem. Eng.*, 52, 150 (1974).

Mathur, K. B., and N. Epstein, *Spouted Beds*, Academic Press, New York (1974).

Schügerl, K., "Experimental Comparison of Mixing Processes in Two- and Three-Phase Fluidized Beds," *Proceedings International Symposium on Fluidization*, p. 782 Netherlands Univ. Press (1967).

Urban, J. C., and A. Gomezplata, "Axial Dispersion Coefficients in Packed Beds at Low Reynolds Numbers," *Can. J. Chem. Eng.*, 47, 353 (1969).

Manuscript received February 3, 1976; revision received and accepted April 12, 1976.

Multiple Minima in a Fluidized Reactor–Heater System

HERBERT T. CHEN

and

L. T. FAN

Department of Chemical Engineering
and
Institute for Systems Design and Optimization
Kansas State University
Manhattan, Kansas 66506

A minimum cost design problem for a single-reaction fluidized-bed reactor system is analyzed in this paper. The problem's mathematical interest stems from Wilde's statements (1974) that there can be only two types of design to this nonlinear, nonconvex, multimodal problem. It is shown by a direct search procedure that, in fact, there are at least four types of optimal design. Furthermore, the type 3, rather than the type 1 design, is the global solution to the numerical example considered in Wilde's work, if the required auxiliary cooler cost is excluded.

SCOPE

This paper examines and discusses a procedure originally suggested by Wilde (1974) for achieving the minimum cost design of a single-reaction fluidized reactor system with feed and recycle heaters. The development of this procedure was based on an extension of Lagrange's method, supplemented by the ideas from geometric programming. It was shown that the globally minimum design necessarily belonged to one of two possible classes of solutions. In an illustrative example involving an exothermic reaction, the type 1 design was then found to be the optimum solution.

The main purpose of the present work is to point out that four types of designs can be found by means of a simple two-dimensional search and that the type 3 design, rather than the type 1 design, is the global solution to the numerical example in which the required cooler cost is excluded. The search procedure is simple to implement, and, unlike Wilde's, it is not necessary to distinguish the solution type in using this procedure. Although attention is focused on a particular second-order exothermic reaction, the procedure can be applied to a wide range of problems. In general, the reaction may be either exothermic or endothermic, of any order, and of any stoichiometric complexity.